Soft Matter b812793j

PAPER

1

Spontaneous symmetry breaking: formation of Janus micelles

Ilja K. Voets,* Remco Fokkink, Thomas Hellweg, Stephen M. King, Pieter de Waard, Arie de Keizer and Martien A. Cohen Stuart

This contribution describes the preparation and solution properties of spontaneously formed ellipsoidal Janus micelles, *i.e.*, non-centrosymmetric nanoparticles, consisting of a disc-like core and cigar-like overall shape *via* co-assembly water-soluble copolymers.

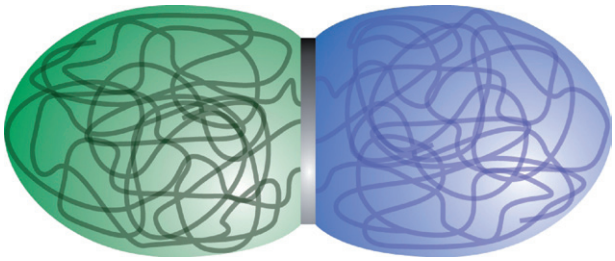

Please check this proof carefully. **Our staff will not read it in detail after you have returned it**.

Translation errors between word-processor files and typesetting systems can occur so the whole proof needs to be read. Please pay particular attention to: tabulated material; equations; numerical data; figures and graphics; and references. If you have not already indicated the corresponding author(s) please mark their name(s) with an asterisk. Please e-mail a list of corrections or the PDF with electronic notes attached – do not change the text within the PDF file or send a revised manuscript.

Please bear in mind that minor layout improvements, e.g. in line breaking, table widths and graphic placement, are routinely applied to the final version.

We will publish articles on the web as soon as possible after receiving your corrections; no late corrections will be made.

Please return your **final** corrections, where possible within **48 hours** of receipt by e-mail to: proofs@rsc.org

Reprints—Electronic (PDF) reprints will be provided free of charge to the corresponding author. Enquiries about purchasing paper reprints should be addressed via: http://www.rsc.org/Publishing/ReSourCe/PaperReprints/. Costs for reprints are below:

Reprint costs

No of pages	Cost for 50 copies	Cost for each additional 50 copies
2–4	£190	£120
5–8	£315	£230
9–20	£630	£500
21–40	£1155	£915
>40	£1785	£1525

Cost for including cover of journal issue:
£55 per 50 copies

Spontaneous symmetry breaking: formation of Janus micelles†

Ilja K. Voets,*[a] Remco Fokkink,[a] Thomas Hellweg,[b] Stephen M. King,[c] Pieter de Waard,[d] Arie de Keizer[a] and Martien A. Cohen Stuart[a]

Received 24th July 2008, Accepted 22nd October 2008
First published as an Advance Article on the web ?????
DOI: 10.1039/b812793j

We describe the preparation and solution properties of Janus micelles, *i.e.*, non-centrosymmetric nanoparticles with compartmentalized shells, *via* co-assembly of two fully water-soluble block copolymers. They consist of a mixed core of poly(*N*-methyl-2-vinyl pyridinium iodide) (P2MVP) and poly(acrylic acid) (PAA), and a shell segregated into two sides, consisting of poly(ethylene oxide) (PEO) or poly(acryl amide) PAAm. These Janus particles form spontaneously and reversibly, *i.e.*, association, dissocation, and reassociation can be carefully controlled *via* parameters, such as polymer mixing fraction, solution p*H*, and ionic strength. Dynamic (polarized and depolarized) and static light scattering, cryogenic transmission electron microscopy, small angle neutron and X-ray scattering, and two-dimensional nuclear magnetic resonance spectroscopy are used to monitor the micellar formation and to characterize the micellar structure. The Janus particles were found to be ellipsoidal, with a cigar-like overall shape and a disc-like core. This peculiar morphology is driven by the delicate interplay between two opposing forces: an attraction between the oppositely charged core blocks and a subtle repulsion between the water-soluble, neutral corona blocks.

1 Introduction

To achieve structural hierarchy from the nanoscopic to the macroscopic level, nature employs a multitude of ways of generating and connecting building blocks, such as covalent bonding, electrostatic interaction, H-bonding, π–π stacking, and so forth, as so elegantly demonstrated by—for example—the living cell and many natural materials, *i.e.*, wood, bone, *et cetera*.[1,2] While covalent bonds play a key role at the smallest length scales, longer range non-covalent interactions dominate at all others. Consider for example a protein molecule. Covalent bonds between individual amino acids yield its primary structure, while its secondary and tertiary structure are mainly governed by non-covalent forces (we note the exception of covalent S–S bonding), such as hydrophobic interactions, H-bonds, and electrostatic interactions. This delicate interplay between various—sometimes opposing—forces gives rise to a three dimensional object with a specific morphology (spheroidal, ellipsoidal, fibrillar) and interaction potential (isotropic or anisotropic), which in turn serves as a building block (or one of the building blocks) for further assembly into yet another level of structural hierarchy.

Hence, it is only natural that chemists, physicists, and material scientists alike, find much of their inspiration in nature. The aim is two-fold: understanding hierarchical assembly in biological systems and applying this knowledge to achieve similar levels of structural hierarchy in purely synthetic systems in a controlled fashion. This has led to the emergence of many new fields of research, including biomineralization and biomimetic mineralization,[3] polypeptide–polymer hybrids,[4–7] de novo synthesis of proteins,[8] protein-like polymers,[9,10] bioengineering,[1,11] and many more. However, nature has one major advantage: millions of years of evolution, leading to an overwhelming amount of variety in building blocks and resulting materials. Another important difference between many natural and synthetic systems is the extent of asymmetry, both in the structure of the (assemblies of) building blocks, as well as in the interactions between them. While the vast majority of (assemblies of) synthetic building blocks is (centro-)symmetric in morphology and/or interaction potential, this is seldom the case for their natural counterparts. Hence, one of the major challenges in current nanotechnology, is the introduction of diversity and asymmetry, *i.e.*, complexity, in synthetic systems. Two main routes can be identified: a chemical and a physical approach. The first focuses on achieving complexity through diversification of the currently available set of building blocks, by advances in chemical synthesis. Significant progress has been made in the field of for example RAFT polymerization[12–14] and de novo protein synthesis,[8] yielding increasingly complicated polymer topologies (*i.e.*, dendrimer, star, gradient, and graft polymers) and monodisperse synthetic analogues of natural proteins with carefully selected properties. The physical route centres around clever combinations of existing building blocks and interactions to achieve the same goal: complexity.

[a]*Laboratory of Physical Chemistry and Colloid Science, Wageningen University, Dreijenplein 6, 6703, HB, Wageningen, The Netherlands. E-mail: ilja.voets@wur.nl; remco.fokkink@wur.nl; arie.dekeizer@wur.nl; martien.cohenstuart@wur.nl*
[b]*Physikalische Chemie I, University of Bayreuth, 95440 Bayreuth, Germany. E-mail: thomas.hellweg@tu-berlin.de*
[c]*ISIS facility, Rutherford Appleton Laboratory, ChiltonDidcot, Oxon, England. E-mail: smk@isise.rl.ac.uk*
[d]*Wageningen NMR Centre, Wageningen University, Dreijenlaan 3, 6703, HA, Wageningen, The Netherlands. E-mail: pieter.dewaard@wur.nl*

† Electronic supplementary information (ESI) available: Experimental details, DLS, SLS, SANS, and SAXS results leading to values for the molar mass, radii, etc., 2D ^{1}H NMR NOESY results (contour plot; line plot at 1.64 ppm), details of the reversible association and dissociation of Janus micelles. See DOI: 10.1039/b812793j

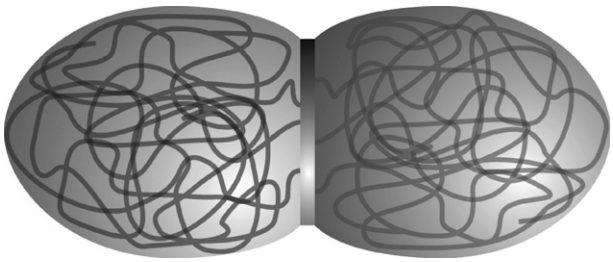

Scheme 1 Schematic representation of a Janus micelle with a prolate ellipsoidal (cigar-like) overall shape and an oblate ellipsoidal (disc-like) core. The core consists of a so-called complex coacervate mesophase in which the PAA and P2MVP blocks are intricately mixed. The corona consists of two segregated domains depicted to the left (PEO) and right (PAAm) of the core. The name Janus particle originates from the Roman deity Janus, the two-faced god of doorways and beginnings.

In this contribution, we illustrate the versatility and simplicity of the latter approach by presenting a completely new route for the preparation of so-called Janus particles, *i.e.*, non-centrosymmetric nanoparticles with compartmentalized shells (Scheme 1). This route circumvents the need for elaborate synthesis procedures and multistep preparation protocols. We will demonstrate that *via* co-assembly of two fully water-soluble coil–coil block copolymers, we are able to prepare such a non-centrosymmetric nanoparticle in a one-step fashion. Furthermore, we will show that, contrary to many chemical routes for the preparation of Janus particles, the particles form spontaneously and reversibly, *i.e.*, association, dissocation, and reassociation can be carefully controlled *via* parameters, such as polymer mixing fraction, solution pH, and ionic strength. A first brief account of our results has recently been published elsewhere.[19]

In light of the recent burst of interest in asymmetric structures and interactions, it is not surprising that Janus particles have attracted much attention.[15–23] Furthermore, they are interesting from a technological point of view, as their composition is thought to render them highly surface-active. It is therefore expected that they may serve as unusually efficient stabilizers of liquid–liquid interfaces, as demonstrated recently for the case of emulsion polymerization[19] and polymer blends.[23] Here, we report on a novel preparation pathway, based purely on equilibrium processes. Hence, the symmetry breaking is achieved spontaneously, and as mentioned previously, in a one-step fashion. To this end, we mix two aqueous solutions of double hydrophilic block copolymers (DHBC),[24] both consisting of a polyelectrolyte block and a neutral block. Thus, we obtain a mixture of molecules that have a tendency towards both an associative and a segregative phase separation. The associative phase separation, a process known as complex coacervation, originates from the electrostatic interaction between the two oppositely charged blocks and from the entropy gain obtained by the counterion release resulting from it. The phenomenon has been intensely investigated since the pioneering works of Tiebackx,[25] Bungenberg de Jong and Kruyt,[26,27] and Voorn and Overbeek,[28] and may be used to drive the formation of so-called complex coacervate core micelles, C3Ms,[21,29–31] also known as polyion complex (PIC) micelles,[32,33] block ionomer complex (BIC) micelles,[34] and interpolyelectrolyte complexes.[35] The segregative phase separation is a result of the subtle repulsion between the chemically different monomers that constitute the neutral blocks, as described by what is known as the Flory–Huggins theory (extended by Scott to describe solutions of two polymers).[36] Both types of phase separation are restricted to the colloidal domain by virtue of the other. As will be shown below, the result of this delicate interplay between opposing forces is the spontaneous formation of polymeric Janus micelles (Scheme 1). In the following, they will be referred to as '(Janus) micelles', '(Janus) particles' and 'C3Ms'. It is clear that they are not centrosymmetric, neither in composition, nor in morphology. Hence, an anisotropic particle is constructed from purely synthetic, relative simple building blocks, which may in turn be used as a building block for further hierarchical structuring, by for example, selectively altering the solvency of one of the neutral blocks in the shell of the particle or upon increasing the micellar volume fraction.

2 Results and discussion

2.1 Preparation of Janus micelles

Upon mixing aqueous solutions of poly(acrylic acid)-*block*-poly(acryl amide), PAA_{42}-*b*-$PAAm_{417}$, and poly(*N*-methyl-2-vinyl pyridinium iodide)-*block*-poly(ethylene oxide), $P2MVP_{42}$-*b*-PEO_{446} under charge stoichiometric conditions (*i.e.*, corresponding to a mixing fraction of P2MVP to P2MVP and PAA monomers, f_+, of 0.5 (pH = 7.7, 1 mM $NaNO_3$), micelles are formed with a molar mass, M_w, of about 500 kg mol^{-1} and a radius, R_h (hydrodynamic radius) and R_g (radius of gyration), of about 18 nm (see Fig. 1, and Fig. S1 and Table S2 in the ESI†). Hence, each micelle consists of about 16–18 diblock copolymers in total, 8–9 of each as $f_+ = 0.5$. As the driving force for the formation of these micelles is electrostatic in nature, pH, ionic strength, and mixing fraction play an important role in their association and dissociation.[29,31,34,35,37] Careful tuning of these parameters to the 'optimal values' (here $f_+ = 0.5$, pH = 7.7, 1 mM $NaNO_3$) is thus necessary to maximize micellar stability and thus aggregation number and size. If the Janus micelles are formed in full thermodynamic equilibrium, their characteristics must be independent of the preparation route. A comparison between three different methods of preparation confirms that this is indeed the case (see Table S4 in the ESI†). In the following sections, we will demonstrate the non-centrosymmetric nature of both the morphology and the composition of these micelles, *i.e.*, their Janus character.

2.2 Characterization of Janus micelles

The first indications that the formed Janus particles may be asymmetric in shape were observed in dynamic light scattering (DLS) experiments (see ESI†). Hence, a thorough investigation with both microscopic and scattering techniques was performed to characterize the particles in detail.

As C3Ms have a tendency to adsorb onto a variety of surfaces, followed by spreading and eventually micellar dissociation while forming a rather homogeneous adsorption layer,[38,39] standard TEM and AFM experiments could not be performed to characterize the Janus particles, as they would dissociate during the sample preparation steps. Thus, we turned to cryogenic transmission electron microscopy (cryo-TEM), for which samples were prepared by rapid vitrification of a solution of Janus

ART ■ B812793J

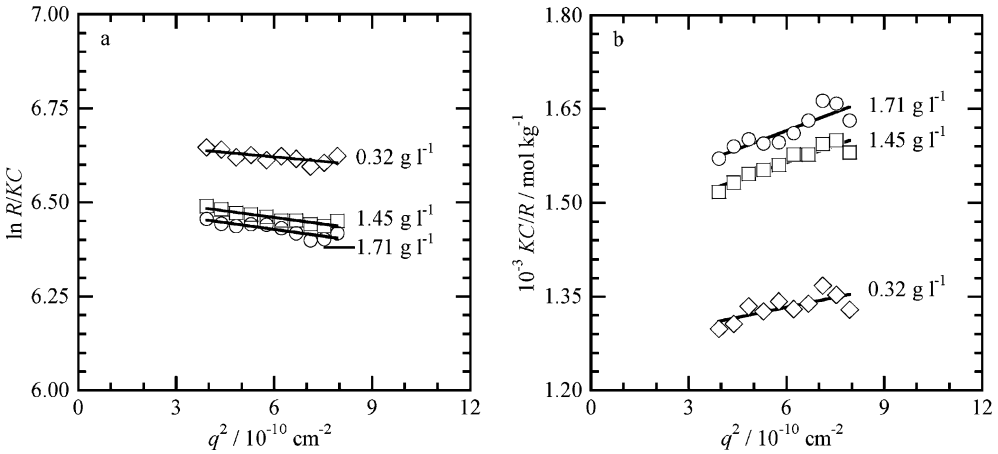

Fig. 1 (a) Guinier representations, ln R/KC versus $q^2/10^{-10}$ cm^{-2} and (b) partial Zimm representations, KC/R versus $q^2/10^{-10}$ cm^{-2} for Janus micelles of PAA_{42}-*b*-$PAAm_{417}$ and $P2MVP_{42}$-*b*-PEO_{446} in H_2O. (○) $C = 1.71$ g l^{-1}, (□) 1.45 g l^{-1}, and (◇) 0.32 g l^{-1}. q-range is $1.98 < q < 2.82\ 10^{-5}$ cm^{-1}. The lines represent fits to the experimental data points. The following abbreviations are used: excess Rayleigh ratio, R, the optical constant, K, the micellar concentration, C, and the magnitude of the scattering wave vector, q.

micelles, so as to preserve the solution structures. The results are shown in Fig. 2. As the micellar corona contributes only marginally in these experiments, due to its low relative polymer volume fraction, we mainly observe the micellar cores. They are visible in the electron micrograph as rather vague light greyish dots, as they are (similar to the micellar corona) highly solvent swollen. While it is clear that no definite conclusions about the shape of the micellar core can be drawn from Fig. 2, the 2D shape irregularity suggests a non-spherical morphology, as projection of a spherical structure into different directions would lead to identical circular images. (Alternative, equally tentative explanations, for the observed irregularity, may be polydispersity and shape fluctuations.) We note that contrary to the particle shape, the particle size is rather constant. The average distance between greyish spots, <d> = 28 ± 3 nm, is close to twice the hydrodynamic radius (~36 nm), while the average spot size of <2*R*> = 20 ± 2 nm and <thickness> = 7 ± 2 nm may be taken as a rough estimate for the core dimensions.

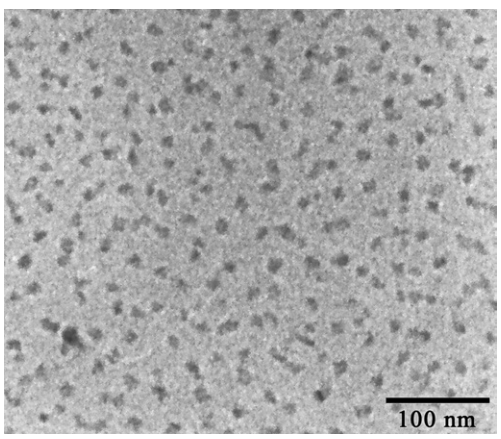

Fig. 2 Cryo-TEM images of a 1:1 mixture of PAA_{42}-*b*-$PAAm_{417}$ and $P2MVP_{42}$-*b*-PEO_{446} in H_2O ($C = 0.97$ g l^{-1}, $f_+ = 0.53$). Adapted with permission from ref. 19.

To complement these results, small angle neutron and X-ray scattering experiments were performed (Fig. 3) in order to study the particle form factor under different contrast conditions. Previously, we have reported SANS measurements on micelles consisting of PAA_{42}-*b*-$PAAm_{417}$ and $P2MVP_{209}$, *i.e.*, in absence of the PAAm block, which were found to be rather polydisperse and spherical in shape.[40] Rather symmetrical pair distance distribution functions were obtained and scattering curves could be modelled well with a form factor for polydisperse, homogeneous spheres (Schulz–Zimm distribution). On the contrary, rather odd-shaped and asymmetrical pair distance distribution functions were obtained for aqueous solutions of PAA_{42}-*b*-$PAAm_{417}$ and $P2MVP_{42}$-*b*-PEO_{446} (Fig. 3), *i.e.*, inconsistent with a (polydisperse) spherical structure. For a flat particle and very small values of r ($r <$ thickness), p(r) will increase quadratically with r, while p(r) will increase linearly with r, for small values of $r >$ thickness.[41] For the micellar cores, which are flattened, but not flat particles, we find such a transition in slope (from steep to less steep) at ~5.7 nm (SAXS) and ~6.7 nm (SANS), *i.e.*, values corresponding nicely to the thickness estimate obtained from the electron micrograph. Based on the GIFT results, we selected a model for polydisperse oblate ellipsoids to describe the scattering data and indeed find an excellent agreement between experimental results and the model (see Fig. S2 in the ESI†). We obtain radii of 15.5 and 1.6 nm from the SAXS model fitting, and 20.0 and 2.2 nm from the SANS model fitting.

Now we have established that the micellar core is indeed rather asymmetric, *i.e.*, the cryo-TEM, SANS, and SAXS experiments are consistent with an oblate ellipsoidal (disc-like) core, we aim to elucidate the overall particle morphology. Depolarised dynamic light scattering (DDLS) measurements have been performed to address this issue. Three modes were observed at $\theta = 30°$, yielding a rotational diffusion coefficient, $D_r \simeq 9400$ Hz, and a translational diffusion coefficient, $D_t \simeq 11.49 \times 10^{-8}$ cm^2 s^{-1} [the third mode presumably corresponds to a (small) number of large (loose) aggregates, see also ESI†]. Rather strikingly, these values are not consistent with the Perrin's equations[42–44] for oblate ellipsoidal particles, and hence, we must conclude that

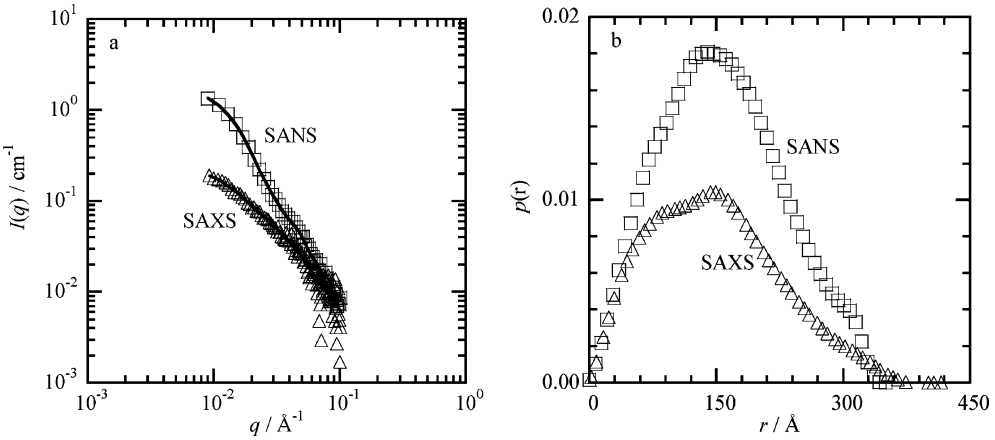

Fig. 3 SANS (□) and SAXS (△) experiments on a 1:1 mixture of PAA_{42}-*b*-$PAAm_{417}$ and $P2MVP_{42}$-*b*-PEO_{446} in D_2O (pD = 7.8, $C = 4.19$ g l^{-1}). (a) Scattering intensity, I(q)/cm^{-1} versus q/$Å^{-1}$. Scattering curves were corrected for solvent scattering. Markers correspond to experimental data; solid lines represent GIFT approximations. (b) Pair distance distribution functions, p(r) versus r/Å. Curves have been normalised to the total area under the curve.

contrary to expectation,[21] the particle core and shell are of different shape. Instead, the values are in agreement with a prolate ellipsoidal (cigar-like) shape of ~45 × 21 × 21 nm. Note the striking similarity in the long (SANS) and small (DDLS) axis values, *i.e.*, 20 and 21 nm respectively. Actually, if one rotates the disc-like core by 90°, it would fit perfectly within the centre of the prolate ellipsoid, segregating the micellar corona into two distinct hemispheres (Scheme 1). Indeed, one may anticipate that such a rare morphology is related to and even induced by the balance between the two opposing forces at play: an attraction between the oppositely charged PAA and P2MVP blocks forcing the two polymers to reside within the same entity, and a repulsion due to the relative immiscibility of the two chemically different coronal blocks PAAm and PEO pushing them to be as far apart as possible.

From PAAm/PEO compatibility studies reported in literature,[45–47] we obtain a rough estimate for the Flory–Huggins interaction parameter, χ of 0.05, based on the equation $\varphi\chi N = 2$ (with the polymer volume fraction, φ, and the degree of polymerisation, N) valid in the critical point. Hence, PAAm and PEO are indeed fairly incompatible and should tend to avoid each other in the micellar corona. To study the proximity of PEO and PAAm chains within the micellar corona directly, two-dimensional proton NMR nuclear Overhauser effect spectroscopy experiments (2D ^{1}H NMR NOESY) were performed (Fig. S3†). Off-diagonal cross-peaks should appear for nearby unlike protons, *i.e.*, within 0.5 nm, as observed previously for C3Ms of PAA_{42}-*b*-$PAAm_{417}$ and $PDMAEMA_{45}$-*b*-$PGMA_{90}$.[48] The circles in Fig. S3† mark the positions where such cross-peaks between the coronal blocks PAAm and PEO should occur. Clearly, no significant peaks are observed. More quantitatively, the area under the intramolecular PAA-*b*-PAAm cross-peaks is about 5–30% of the corresponding diagonal peak, while nothing > 0.2% is observed at the encircled positions (Fig. S4†). As PEO and PAAm are both highly flexible, we may conclude that the blocks indeed avoid each others presence, *i.e.*, PEO and PAAm chains tend to segregate.

The complete characterization of the Janus micelles is graphically summarized in Scheme 1. We postulate that the observed two-fold elliptical morphology, disc-like for the core and cigar-like for the corona, is a direct consequence of the delicate interplay between several opposing forces, *i.e.*, the attraction between the core-forming P2MVP and PAA blocks, and the repulsion between the corona-forming PEO and PAAm blocks. Indeed, spherical morphology is observed in C3Ms of identical composition (P2MVP, PAA, PEO) in absence of PAAm.[40,49] Thus, if cleverly combined relatively simple building blocks can give rise to complicated hierarchical assemblies. A subsequent publication will report on the systematic investigation of several factors that influence particle asymmetry and coronal heterogeneity.[50] We presume that the coronal volume fraction of EO and AAm monomers, the polymerisation degree of the PAAm and PEO blocks, the core–corona interfacial tension, the tendency towards local charge compensation dictating intricate mixing of PAA and P2MVP blocks, are just a few of the relevant parameters.

2.3 Reversible association and dissociation of Janus micelles

Many authors have demonstrated the reversible nature of the association and dissociation of oppositely charged polymers into centrosymmetric micelles, C3Ms, upon changes in mixing fraction, ionic strength, and pH.[29,31,34,35,37] In the above, we have shown that a delicate balance between 'frustrated' (in terms of domain size) associative and segregative phase separation can be applied to yield non-centrosymmetric Janus particles in a one-step fashion. Now, we will demonstrate that the reversibility of the micellar formation, inherent to the moderate driving force, *i.e.*, electrostatic interaction, is preserved.

Light scattering theory (see eqn 2–5 in the ESI†) tells us that an increase in scattering intensity at 90° normalized by the particle concentration, $I_{90°}/C$, is directly related to an increase in particle mass and aggregation number, assuming the particle form and structure factor to be unity, *i.e.*, $P(q)$, $S(q) \approx 1$, and the differential refractive index, dn/dc to be constant (*i.e.*, in the following, independent of f_+). Hence, in Fig. 4 we observe an increase in particle mass upon addition of an aqueous solution of $P2MVP_{42}$-*b*-PEO_{446} to a solution of PAA_{42}-*b*-$PAAm_{417}$, *i.e.*, upon

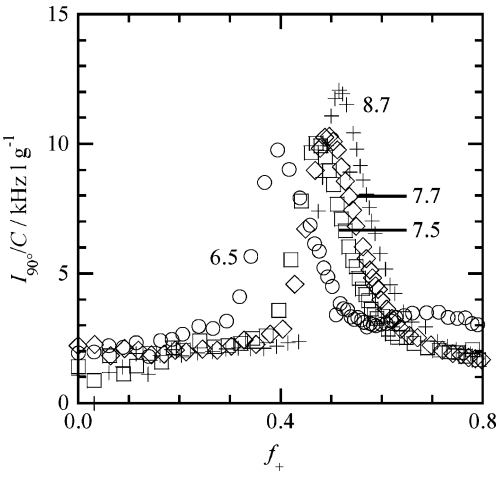

Fig. 4 $I_{90°}/C$/kHz l g^{-1} as a function of mixing fraction, f_+, for mixtures of PAA_{42}-*b*-$PAAm_{417}$ and $P2MVP_{42}$-*b*-PEO_{446} (C = 0.99–3.26 g l^{-1}) at $pH_+ = pH_- = (\bigcirc)$ 6.5, $(\square)$ 7.5, $(\diamond)$ 7.7, and (+) 8.7. pH_+ corresponds to the pH of the $P2MVP_{42}$-*b*-PEO_{446} stock solution; pH_- corresponds to the pH of the PAA_{42}-*b*-$PAAm_{417}$ stock solution.

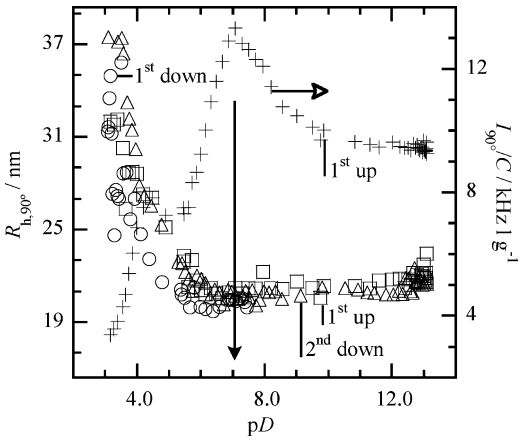

Fig. 5 $I_{90°}/C$/kHz l g^{-1} and $R_{h,\,90°}$ (cumulant analysis) as a function of pD for a 1:1 mixture of PAA_{42}-*b*-$PAAm_{417}$ and $P2MVP_{42}$-*b*-PEO_{446} (f_+ = 0.49, C = 0.82–1.01 g l^{-1}, D_2O). Left axis: $R_{h,\,90°}$/nm ($\bigcirc$: 1st pH decrease; $\square$: 1st pH increase, $\triangle$: 2nd pH decrease); right axis: $I_{90°}/C$/kHz l g^{-1} (+: 1st pH increase). Four pH cycles were performed, three pH cycles are shown for reasons of clarity. The open arrow indicates the axis for the $I_{90°}/C$/kHz l g^{-1} versus pH curve. The closed arrow indicates the pD at maximum $I_{90°}/C$, which is 6.7. The ionic strength increases about 14 mM during the experiment due to acid/base addition.

increasing f_+ for low values of f_+, and a decrease in average particle mass upon increasing f_+ for high values of f_+. The maximum is known as the preferred micellar composition, PMC, which is defined as the mixing fraction where most micelles are formed.[30,31] Hence, the polymers spontaneously associate into Janus micelles under charge-stoichiometric conditions (for example, $f_+ = 0.5$, pH = 7.7, 1 mM $NaNO_3$) and dissociate upon over-titration with either polymer, that is, upon addition of extra charge in the form $P2MVP_{42}$-*b*-PEO_{446} (high values of f_+) and PAA_{42}-*b*-$PAAm_{417}$ (low values of f_+).

In Fig. 4, $I_{90°}/C$/kHz l g^{-1} is plotted as a function of mixing fraction, f_+, for different initial pH values. Clearly, the Janus micelles reversibly associate and dissociate upon increasing f_+ and furthermore, the position of the PMC is pH dependent as the polyacid block in PAA_{42}-*b*-$PAAm_{417}$ (and the non-quaternized P2VP segments within the $P2(M)VP_{42}$-*b*-PEO_{446} copolymer) is a weak polyelectrolyte.[30,31] As the charge density of PAA_{42}-*b*-$PAAm_{417}$ increases with increasing pH, the PMC shifts to higher values of f_+, as more $P2MVP_{42}$-*b*-PEO_{446} polymers are necessary to reach charge neutrality (see Table S5 in the ESI†). As the particles are the most stable when charge stoichiometry is reached at exactly $f_+ = 0.5$, all experiments were performed with polymer stock solutions prepared at pH = 7.7.

As C3Ms are most stable under charge neutral conditions, *i.e.*, $\alpha_- f_- = \alpha_+ f_+$ (α denotes the degree of dissociation), micellar stability depends on both mixing fraction and the degree of dissociation, which is pH dependent in case of weak polyelectrolyte blocks (as was shown above). In fact, C3Ms composed of two oppositely charged polymers, both containing weak polyelectrolyte blocks, reversibly dissociate above and below a certain critical pH, when either α_- or α_+ is below the minimum required value for micellization. Thus, we now employ pH to tune the charge balance, and demonstrate that again, the Janus micelles can reversibly associate and dissociate. Note however, that the Janus micelles are composed of two diblock copolymers, one containing a weak polyelectrolyte block, PAA_{42}-*b*-$PAAm_{417}$, and one containing a polyelectrolyte block that is partially quaternised, $P2MVP_{42}$-*b*-PEO_{446}, *i.e.*, its charge is only partially pH dependent. Hence, they are expected to dissociate at low pH, but may remain stable (enough) at high pH.

Fig. 5 shows $R_{h,\,90°}$/nm and $I_{90°}/C$/kHz l g^{-1} as a function of pD (experiment was performed in D_2O). The observed variations in $R_{h,\,90°}$ and $I_{90°}/C$ with pD are explained as follows. Again, we observe a maximum in $I_{90°}/C$ at a certain position, now corresponding to the preferred pD, pD_{max}, for $f_+ = 0.49$. For pD < pD_{max} and pD > pD_{max}, we observe a decrease in $I_{90°}/C$, *i.e.*, (partial) dissociation of the Janus micelles. Rather strikingly, both $I_{90°}/C$ and $R_{h,\,90°}$ show a dependence on pD that is asymmetric with respect to pD_{max}. For pD > 5.7, $R_{h,\,90°}$ has a rather constant value of 20.8 ± 2.2 nm, while $I_{90°}/C$ reaches a maximum value at 6.7. For pD < 5.7, $R_{h,\,90°}$ is no longer constant, while $I_{90°}/C$ decreases with decreasing pD. Apparently, Janus micelles are present at intermediate to high values of pD (5.7 < pD < 12.9), the maximum amount of micelles occurs at pD = 6.7, and no Janus particles exist at low pD, *i.e.*, below ~5.7. Note however that an alternative explanation for the existence of micelles under basic conditions, may be the self-assembly of $P2MVP_{42}$-*b*-PEO_{446} copolymers (*i.e.*, in coexistence with unimerically dissolved PAA_{42}-*b*-$PAAm_{417}$ copolymers), as micellization is observed in aqueous solutions of non-quaternised P2VP-*b*-PEO for pH > 6.1.[35] The increase in $R_{h,\,90°}$ for pD < 5.7 is counterintuitive, as C3Ms dissociate into soluble complexes consisting of a few polymers and free $P2MVP_{42}$-*b*-PEO_{446} polymers, which one naturally presumes to be smaller in size as both have a smaller mass and aggregation number than the C3Ms. However, we obtained $R_{h,\,90°}$ = 45.4 ± 9.8 nm ($I_{90°}/C$ = 0.72 ± 0.09 kHz l g^{-1}) for an independent light scattering experiment on an aqueous $P2MVP_{42}$-*b*-PEO_{446} solution (D_2O, 2.7 < pD < 12.5), and $R_{h,\,90°}$ = 10.5 ± 1.8 nm ($I_{90°}/C$ = 0.78 ± 0.04 kHz l g^{-1}) for an aqueous PAA_{42}-*b*-$PAAm_{417}$ solution (3.9 < pH < 12.6). Hence, due to the large $R_{h,\,90°}$ of $P2MVP_{42}$-*b*-PEO_{446} in aqueous

solution, the dissociation of Janus micelles can indeed lead to the observed increase in $R_{h,\ 90^\circ}$ for pH < 5.7. We note that presently, the origin of the shoulder in the I_{90°/C versus pH curve for 4 < pH < 5.7 is not understood and warrants further investigation. We may speculate that it is related to the formation of hydrogen bonds between AA and AAm units of PAA_{42}-*b*-$PAAm_{417}$, as both I_{90°/C and $R_{h,\ 90^\circ}$ were found to increase for pH < 3.9 in aqueous solutions of PAA_{42}-*b*-$PAAm_{417}$ in absence of $P2MVP_{42}$-*b*-PEO_{446} (data not shown). In conclusion, we note that the association and dissociation of Janus micelles is reversible with respect to pD, as nearly equal values of I_{90°/C and $R_{h,\ 90^\circ}$ are obtained for a given pD in subsequent pD cycles.

Finally, Fig. 6 demonstrates the dissociation of Janus micelles upon increasing ionic strength. Indeed, the existence of a so-called critical ionic strength, I_{cr}, being the ionic strength above which C3Ms can no longer be observed, has been reported many times in the literature,[34,35,37,51] and may be used for various practical purposes, such as an on-off switch of enzymatic catalysts.[37] It is a consequence of the increased charge screening upon increasing ionic strength, which diminishes the strength of the electrostatic interactions, affecting the stability of the micelles. For Janus micelles in H_2O and D_2O, we find a critical value of $[NaNO_3] = 0.34$ M. The hydrodynamic radius is found to decrease with increasing ionic strength to a constant value of 7.4 ± 0.5 nm.

Note that we have not presented direct measurements proving that the Janus-type morphology is preserved under all conditions (ionic strength, pH, mixing fraction). We address this issue in detail in an upcoming publication, where we systematically investigate the influence of several important factors, such as the ionic strength and PEO/PAAm mixing fraction, on particle asymmetry and coronal heterogeneity.[50] Based on those investigations, we concluded that the Janus-type segregation in the present system appears rather robust; *i.e.*, experimental conditions corresponding to a transition towards a heterogeneous corona were not observed.

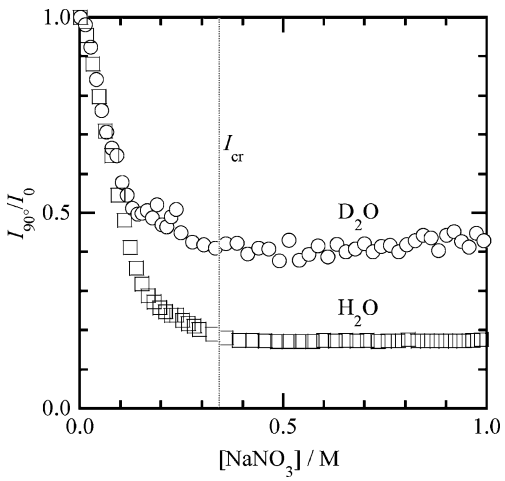

Fig. 6 Addition of $NaNO_3$ leads to a dissociation of Janus micelles (□: H_2O, $f_+ = 0.50$, $C = 7.22$–10.01 g l^{-1}, pH = 7.7; ○: D_2O, $f_+ = 0.50$, $C = 7.41$–10.22 g l^{-1}, pH = 7.7). Results are given as the normalised light scattering intensity, I_{90°/I_0 versus $[NaNO_3]$/M. The line indicates the critical ionic strength, I_{cr}, corresponding to $[NaNO_3] = 0.34$ M. Note that solvent scattering has not been subtracted.

3 Conclusions

In the above, we have shown that a clever combination of simple building blocks and opposing non-covalent interaction forces, achieved *via* the co-assembly of two fully water-soluble double hydrophilic block copolymers [poly(*N*-methyl-2-vinyl pyridinium iodide)-*block*-poly(ethylene oxide), $P2MVP_{42}$-*b*-PEO_{446} and poly(acrylic acid)-*block*-poly(acryl amide), PAA_{42}-*b*-$PAAm_{417}$], gives rise to spontaneous symmetry breaking within a polymer micelle. Structural complexity is realized in the form of a non-centrosymmetric Janus micelle as depicted schematically in Scheme 1. The core and shell are both ellipsoidal, the former being disc-like (oblate ellipsoidal), the latter being cigar-like (prolate ellipsoidal). Furthermore, while the core segments (PAA and P2MVP) are intrinsically mixed, the corona segments (PEO and PAAm) tend to avoid each other as much as possible. Such a nanoparticle is the equilibrium result of a delicate balance between an associative phase separation (attraction between PAA and P2MVP segments) and a segregative phase separation (subtle repulsion between PEO and PAAm), both restricted to the colloidal domain by virtue of the other. We have also shown that the particles are 'multi-responsive', *i.e.*, they reversibly associate and dissociate in response to changes in mixing fraction, pH, and ionic strength. In future work, analytical ultracentrifugation might be employed to allow for a more detailed insight into the aggregation behaviour[52] such as the dynamics of aggregation/deaggregation.

It is our expectation that other combinations of opposing non-covalent interactions will similarly lead to asymmetric structures. Furthermore, one may also employ kinetically controlled processes (as opposed to equilibrium processes), the combination of which may introduce a temporal sequence, as is the case in *e.g.* protein folding, which can be exploited to achieve further complexity. We anticipate that sequential assembly of these Janus micelles into higher order structures (mediated by, *e.g.*, an increase in the micellar volume fraction or a decrease in the solvency of one of the neutral blocks) will be directional and will thus give rise to structural ordering on yet another length scale, provided of course, that its anisotropic nature, as well as the proper balance between all driving forces, is maintained.

Acknowledgments

We thank ISIS for providing the beam time and R. K. Heenan, A. E. Terry, and D. Visser for help and NWO for financial support. We thank Gert Buurman for the creation of Scheme 1. We thank Peter M. Frederik and Paul H. H. Bomans for the Cryo-TEM experiments, Kurt Stubenrauch, Gerhard Fritz, and Otto Glatter for the SAXS experiments. This work is part of the research programme of the Stichting voor Fundamenteel Onderzoek der Materie (FOM), which is financially supported by the Nederlandse Organisatie voor Wetenschappelijk Onderzoek (NWO). It has been carried out in the framework of the EU Polyamphi/Marie Curie program (FP6-2002, proposal 505027). IV was financed by the SONS Eurocores program (Project JA016-SONS-AMPHI). Holger Schmalz is gratefully acknowledged for the synthesis of the P2MVP-*b*-PEO polymer and Rhodia for providing us with a sample of PAA-*b*-PAAm.

References

1 P. Fratzl and R. Weinkamer, *Prog. Mater. Sci.*, 2007, **52**(8), 1263–1334.
2 J. Aizenberg, J. C. Weaver, M. S. Thanawala, V. C. Sundar, D. E. Morse and P. Fratzl, *Science*, 2005, **309**(5732), 275–278.
3 A. W. Xu, Y. R. Ma and H. Colfen, *J. Mater. Chem.*, 2007, **17**(5), 415–449.
4 J. M. Smeenk, L. Ayres, H. G. Stunnenberg and J. C. M. van Hest, *Macromol. Symp.*, 2005, **225**, 1–8.
5 H. A. Klok, *J. Polym. Sci. Part A: Polym. Chem.*, 2005, **43**(1), 1–17.
6 H. Schlaad and M. Antonietti, *Eur. Phys. J. E*, 2003, **10**(1), 17–23.
7 H. G. Borner, B. M. Smarsly, J. Hentschel, A. Rank, R. Schubert, Y. Geng, D. E. Discher, T. Hellweg and A. Brandt, *Macromolecules*, 2008, **41**(4), 1430–1437.
8 A. Ohta, Y. Yamagishi and H. Suga, *Curr. Opin. Chem. Biol.*, 2008, **12**(2), 159–167.
9 A. R. Khokhlov, A. N. Semenov and A. V. Subbotin, *Eur. Phys. J. E*, 2005, **17**(3), 283–306.
10 A. R. Khokhlov and P. G. Khalatur, *Curr. Opin. Solid State Mater. Sci.*, 2004, **8**(1), 3–10.
11 P. Fratzl, *Curr. Opin. Colloid Interface Sci.*, 2003, **8**(1), 32–39.
12 G. Moad, E. Rizzardo and S. H. Thang, *Polymer*, 2008, **49**(5), 1079–1131.
13 L. Barner, T. P. Davis, M. H. Stenzel and C. Barner-Kowollik, *Macromol. Rapid Commun.*, 2007, **28**(5), 539–559.
14 W. A. Braunecker and K. Matyjaszewski, *Prog. Polym. Sci.*, 2007, **32**(1), 93–146.
15 T. Higuchi, A. Tajima, H. Yabu and M. Shimomura, *Soft Matter*, 2008, **4**(6), 1302–1305.
16 B. Liu, W. Wei, X. Z. Qu and Z. H. Yang, *Angew. Chem., Int. Ed.*, 2008, **47**(21), 3973–3975.
17 F. Wurm, H. M. Konig, S. Hilf and A. F. M. Kilbinger, *J. Am. Chem. Soc.*, 2008, **130**(18), 5876, –+.
18 A. Walther and A. H. E. Muller, *Soft Matter*, 2008, **4**(4), 663–668.
19 A. Walther, M. Hoffmann and A. H. E. Muller, *Angew. Chem., Int. Ed.*, 2008, **47**(4), 711–714.
20 P. G. Degennes, *Rev. Mod. Phys.*, 1992, **64**(3), 645–648.
21 I. K. Voets, A. de Keizer, P. de Waard, P. M. Frederik, P. H. H. Bomans, H. Schmalz, A. Walther, S. M. King, F. A. M. Leermakers and M. A. Cohen Stuart, *Angew. Chem., Int. Ed.*, 2006, **45**(40), 6673–6676.
22 A. Walther, X. Andre, M. Drechsler, V. Abetz and A. H. E. Müller, *J. Am. Chem. Soc.*, 2007, **129**(19), 6187–6198.
23 A. Walther, K. Matussek and A. H. E. Mueller, *ACS Nano*, 2008, **2**(6), 1167–1178.
24 H. Colfen, *Macromol. Rapid Commun.*, 2001, **22**(4), 219–252.
25 F. W. Tiebackx, *Zeitschrift fur Chemie und Industrie der Kolloide*, 1911, **8**, 198–201.
26 H. G. Bungenberg de Jong, Complex colloid systems, in *Colloid Science*, ed. Kruyt, H. R., Elsevier, Amsterdam, 1949, vol. II, (ch. X).
27 H. G. Bungenberg de Jong and H. R. Kruyt, *Proceedings of the Koninklijke Nederlandse Akademie van Wetenschappen*, 1929, **32**, 849–856.
28 J. T. G. Overbeek and M. J. Voorn, *J. Cell. Comparative Physiol.*, 1957, **49**(S1), 7–26.
29 M. A. Cohen Stuart, B. Hofs, I. K. Voets and A. de Keizer, *Curr. Opin. Colloid Interface Sci.*, 2005, **10**(1–2), 30–36.
30 S. van der Burgh, A. de Keizer and M. A. Cohen Stuart, *Langmuir*, 2004, **20**(4), 1073–1084.
31 B. Hofs, I. K. Voets, A. de Keizer and M. A. Cohen Stuart, *Phys. Chem. Chem. Phys.*, 2006, **8**(36), 4242–4251.
32 A. Harada and K. Kataoka, *Macromolecules*, 1995, **28**(15), 5294–5299.
33 A. Harada and K. Kataoka, *Science*, 1999, **283**(5398), 65–67.
34 A. V. Kabanov, T. K. Bronich, V. A. Kabanov, K. Yu and A. Eisenberg, *Macromolecules*, 1996, **29**(21), 6797–6802.
35 J. F. Gohy, S. K. Varshney, S. Antoun and R. Jerome, *Macromolecules*, 2000, **33**(25), 9298–9305.
36 R. L. Scott, *J. Chem. Phys.*, 1949, **17**(3), 279–284.
37 A. Harada and K. Kataoka, *J. Am. Chem. Soc.*, 1999, **121**(39), 9241–9242.
38 S. van der Burgh, R. Fokkink, A. de Keizer and M. A. Cohen Stuart, *Colloids Surf. A: Physicochem. Eng. Aspects*, 2004, **242**(1–3), 167–174.
39 I. K. Voets, W. A. de Vos, B. Hofs, A. de Keizer, M. A. Cohen Stuart, R. Steitz and D. Lott, *J. Phys. Chem. B*, 2008, **112**(23), 6937–6945.
40 I. K. Voets, S. van der Burgh, B. Farago, R. Fokkink, D. Kovacevic, T. Hellweg, A. de Keizer and M. A. Cohen Stuart, *Macromolecules*, 2007, **40**(23), 8476–8482.
41 P. Lindner and T. Zemb, *Neutron, X-Rays and Light: Scattering Methods Applied to Soft Condensed Matter*, Elsevier, Amsterdam, 2002.
42 F. Perrin, *J. Phys. Radium*, 1934, **5**, 497–511.
43 F. Perrin, *J. Phys. Radium*, 1936, **7**, 1–11.
44 B. J. Berne and R. Pecora, *Dynamic Light Scattering*,Dover Publications, Inc., New York, 2000.
45 M. Silva, J. C. Machado, V. Mano and G. G. Silva, *J. Polym. Sci. Part B: Polym. Phys.*, 2003, **41**(13), 1493–1500.
46 R. J. Hefford, *Polymer*, 1984, **25**(7), 979–984.
47 M. B. Perrau, I. Iliopoulos and R. Audebert, *Polymer*, 1989, **30**(11), 2112–2117.
48 I. K. Voets, A. de Keizer, M. A. Cohen Stuart and P. de Waard, *Macromolecules*, 2006, **39**(17), 5952–5955.
49 I. K. Voets, R. de Vries, R. Fokkink, J. Sprakel, R. May, A. de Keizer and M. A. Cohen Stuart, *J. Phys. Chem. B*, 2008, , submitted.
50 I. K. Voets, R. Fokkink, A. de Keizer, R. May, P. de Waard and M. A. Cohen Stuart, *Langmuir*, 2008, , accepted.
51 M. A. Cohen Stuart, N. A. M. Besseling and R. G. Fokkink, *Langmuir*, 1998, **14**(24), 6846–6849.
52 N. Karibyants, H. Dautzenberg and H. Colfen, *Macromolecules*, 1997, **30**(25), 7803–7809.

ART ■ B812793J

Authors Queries

Journal: **SM**

Paper: **b812793j**

Title: **Spontaneous symmetry breaking: formation of Janus micelles**

Editor's queries are marked like this... **1**, and for your convenience line numbers are inserted like this... 5

Query Reference	Query	Remarks
1	For your information: You can cite this article before you receive notification of the page numbers by using the following format: (authors), Soft Matter, 2008, DOI: 10.1039/b812793j.	
2	"unimerically" is not a word, do you mean "monomer-dissolved"?	